

The Role of Edge parameters for L-H Transitions and ELM Behaviour on ASDEX Upgrade

W. Suttrop, H. J. de Blank, G. Haas, H. Murmann, O. Gehre, H. Reimerdes, F. Rytter, H. Salzmann, J. Schweinzer, J. Stober, H. Zohm, ASDEX Upgrade team, NBI team, ICRH team, Max-Planck-Institut für Plasmaphysik, EURATOM Association, D-85748 Garching

Introduction

Local plasma parameters play an important role for transition to high-confinement mode (H-mode) since loss mechanisms which drive the radial electrical field associated with improved confinement [1] critically depend on collisionality and ion temperature and density gradient lengths at the plasma edge. However, partly due to diagnostic difficulties, the clearest picture of L- to H-mode transitions exists so far with respect to global quantities [2, 3]. Few measurements of local parameters have been reported as yet, including an early observation of constant T_e at L-H and H-L transitions on ASDEX [4]. More recent results of JET [5] and of a parameter scan on DIII-D [6] agree on the role of edge temperature as a critical parameter but are ambiguous about the dependence on B_t . Edge Localized Modes (ELMs), always observed during stationary H-mode, impose a stability limit on the edge pressure gradient, but ELM parameters (e.g. ELM type) themselves depend on edge conditions.

Here, we report local T_e , T_i and n_e measurements made at the plasma edge of ASDEX Upgrade at L-H and H-L transitions and ELMs in an attempt to describe the local edge parameter space of L-mode, L-H transitions, and H-mode with various ELM types. A detailed quantitative comparison of edge T_i , n_e , T_e profiles and neutral flux measurements with transition theory for a limited number of discharges is addressed in a separate paper [7].

For the present investigation, a set of 98 discharges is randomly selected from recent ASDEX Upgrade deuterium discharges with similar geometry (lower single null, ion- ∇B direction towards the X-point, $R = 1.65$ m, $a = 0.5$ m, elongation $\kappa \approx 1.7$, triangularity $\delta \approx 0.07$). Varying discharge parameters are $B_t = 1.5 \dots 3$ T, $I_p = 0.6 \dots 1.2$ MA, $P_{NBI} = 2.5 \dots 7.5$ MW, and $P_{ICRF} = 0 \dots 2$ MW. The set contains shots with and without Neon impurity gas puff. Diagnostics include DCN FIR laser interferometry and Li beam for density measurements, 16-channel Thomson scattering and 45-channel ECE radiometry for electron temperature measurements, and two ionization gauges installed near the divertor and in the main chamber to measure the neutral gas flux.

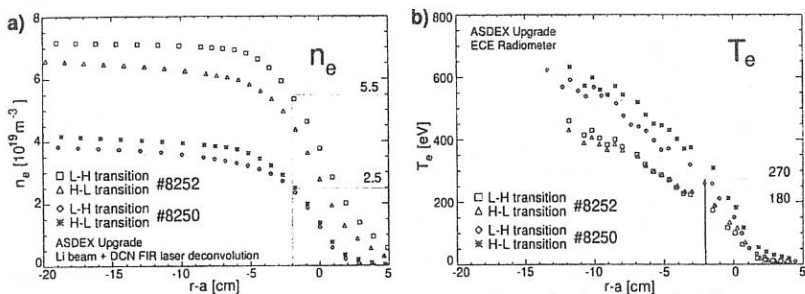


Figure 1: Comparison of L-H and H-L transitions of two discharges with different line averaged density a) electron density b) electron temperature profiles

L-H and H-L transitions

We first consider an example to illustrate the relevance of local parameters at the L-H and H-L thresholds. Fig. 1 shows a pair of discharges (ASDEX Upgrade #8250, #8252) with electron density varied and otherwise identical parameters ($B_t = 2.5$ T, $I_p = 1.0$ MA). Slow L-H transitions are achieved by switching a 2.5 MW neutral beam at 34 Hz rate. Line averaged densities (in 10^{19} m^{-3}) / NBI duty cycles at the L-H and H-L transitions are 3.9/50% (#8250, L-H), 7/100% (#8252, L-H), 4/30% (#8250, H-L), and 6.4/30% (#8252, H-L). Edge densities of the two discharges differ by a factor of 2.5 (Fig.1 a). The edge electron temperature (Fig.1 b), taken at 2 cm inside the nominal separatrix, differs by 50% for the two shots, where a higher temperature is found at lower density. The difference in T_e between L-H and H-L transitions is small, of the order of few percent, with the tendency of lower ratio T_e/n_e at L-H compared to H-L.

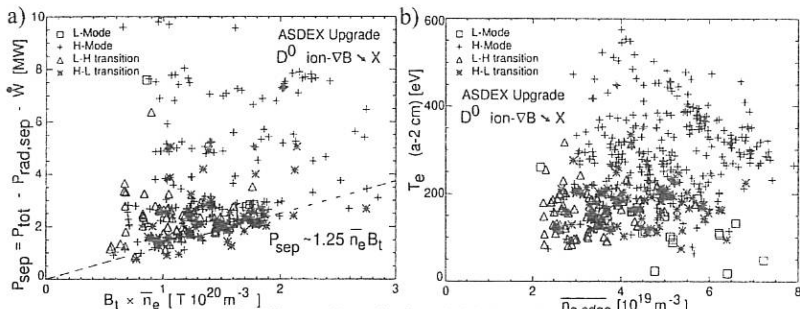


Figure 2: Comparison of different H-mode threshold dependencies: a) P_{sep} vs. $\bar{n}_e B_t$. b) T_e (edge) vs. \bar{n}_e (edge)

We now compare the global scaling of $P_{sep} = P_{tot} - dW/dt - P_{rad,sep}$ with the dependence of edge T_e on edge density for the set of 98 recent discharges characterized above. Fig. 2 a) shows P_{sep} as a function of $\bar{n}_e B_t$ for L-H, H-L transitions, stationary H-mode, and few L-mode phases with auxiliary heating. The dashed line represents the scaling of P_{sep} (MW) = $1.25 \bar{n}_e (10^{20} \text{ m}^{-3}) B_t$ (T) derived from earlier ASDEX Upgrade discharges [8]. Although there is a fair agreement with the global $\bar{n}_e B_t$ -scaling, several data points depart, which probably reflects the difficulties to determine accurately the fraction of power radiated from inside the separatrix and dW/dt during fast changes of heating power. Fig. (Fig. 2 b) shows a plot of edge electron temperature T_e at $r = a - 2$ cm (obtained by interpolation of two adjacent Thomson channels) vs. edge line-averaged density $\bar{n}_{e,edge}$ for the same data set. A radial position 2 cm (corresponding to $\rho_p = 0.97$) inside the nominal separatrix is selected, because it is believed to be relevant for transition physics but sufficiently distant from the separatrix to avoid T_e being entirely determined by the heat flux to the divertor. There is a large scatter in the T_e data, but no significant dependence on $\bar{n}_{e,edge}$ and also no significant difference in T_e for L-H and H-L transitions is observed. Values of $T_e(r = a - 2 \text{ cm})$ at the transition center around ≈ 160 eV, with T_e above during H-mode and below during L-mode. H- and L-modes can exist over the entire experimental edge density range of $2 \dots 7 \times 10^{19} \text{ m}^{-3}$.

At high neutral densities (main chamber neutral flux $\Gamma_0 \geq 5 \times 10^{21} \text{ m}^{-2} \text{ s}^{-1}$). L-modes are

obtained even for high heating power ($P_{tot} = 8$ MW). This illustrates that H-mode can be inaccessible above certain neutral densities. However, since these discharges also have high n_e , high bulk radiation and low edge T_e , it is not exactly clear which mechanism causes this effect.

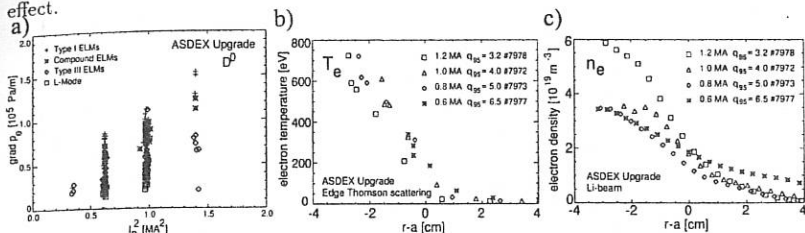


Figure 3: Scaling of the edge pressure gradient with plasma current: a) $\nabla p_e(I_p^2)$ for a set of discharges, b) edge T_e and c) n_e profiles measured for q_a varied by I_p variation.

Edge Localized Modes

Following the DIII-D classification [9], ELMs of type I and III are observed on ASDEX Upgrade [10]. In addition, compound ELMs exist which are identified as ELM events with subsequent brief transition to L mode [11]. As for pressure gradient driven instabilities, one would expect that edge n_e, T_e profiles reflect the stability limit of type I ELMs at [12, 10] and type III ELMs below the ideal ballooning limit [13]. In the first stability region at high shear or in the cylindrical approximation, the normalized pressure gradient $\alpha = 2\nabla p \mu_0 R q^2 / B_i^2$ at the ideal ballooning limit is approximately proportional to the normalized shear $S = (dq/dr) \times (r/q)$ [14]. Assuming that S is approximately independent of q_a , one would expect the maximum $\nabla p = \nabla p_{crit}$ to be proportional to I_p^2 and independent of B_i . This is indeed observed for the set of discharges as shown in Fig. 3 a). For given I_p , highest pressure gradients are observed during type I ELMs H-mode. Pressure gradients in phases with type III ELMs are significantly lower but still above ∇p_e in L-mode. An I_p -scan (Fig. 3 b, c) with otherwise identical parameters ($P_{NBI} = 5$ MW, $B_i = 2.5$ T) reveals that the change in ∇p is almost entirely due to different edge densities, while edge T_e profiles change much less with I_p , consistent with expectation that $\tau_p \propto I_p$. For all discharges except at $I_p = 0.6$ MA gas puff was switched off during H-mode.

Apart from stability limits imposed by ELMs on the edge pressure gradient, the occurrence of the various ELM types can be parametrized by local edge quantities. Fig. 4 a) shows the edge electron pressure gradient normalized to I_p^2 vs. T_e at $r = a - 2$ cm for the set of discharges in deuterium. Type I ELMs mainly populate the region above $\nabla p_e / I_p^2 = 1.5 \times 10^5$ Pa/m/MA² and $T_e(a - 2\text{cm}) \approx 300$ eV while type III ELMs predominate below. From a plot of T_e vs. n_e at $r = a - 2$ cm (Fig. 4 b) one sees that type III ELMs occur at lower T_e than type I ELMs but both types are observed independent of density. At high resistivity, type III ELMs are destabilized at lower pressure gradient than type I ELMs, while at low resistivity, the fixed stability limit of type I ELMs is reached first, consistent with the picture of a resistive instability [11]. Compound ELMs appear mainly at high edge density (or high neutral gas flux, which is correlated), regardless of B_i , which varies by a factor of 2 in the set. They are found either at intermediate or at low pressure gradient, and can therefore be attributed to type I ELMs or type III ELMs, respectively, followed by a brief L-mode period.

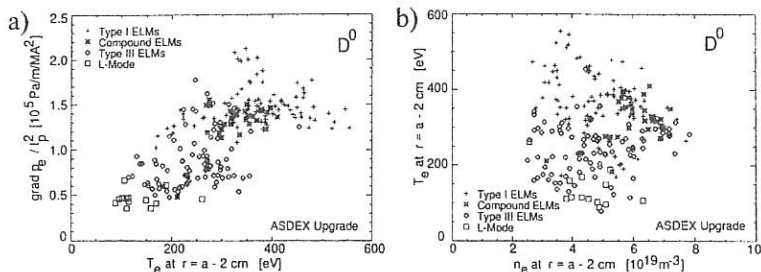


Figure 4: Occurrence of various ELM types a) $\nabla p_e / I_p^2$ vs. T_e and b) T_e vs. n_e

Conclusion

On ASDEX Upgrade, T_e at the edge at L-H and H-L transitions is found to be independent of a number of plasma parameters, in particular P_{tot} , B_t , I_p , although there is considerable scatter ($\pm 30\%$) in the data set. Also, no density dependence is obvious from the data set. However, comparison of individual discharges shows that T_e and T_i decrease by $\approx 50\%$ when the edge density is raised by a factor of 2.5. This finding indicates a possible weak dependence of T_e and T_i on density, but also implies that L-H transitions are obtained at very different edge collisionalities. More detailed measurements are necessary to check whether the departure from constant T_e found on other experiments [4, 6] is significant. There is only a weak difference of T_e at the L-H and H-L transitions, indicating that the hysteresis in P_{tot} is owed mainly to the change in confinement. At highest neutral densities, the H-mode is quenched even at high heating powers. This may indicate that an upper limit to neutral densities in H-mode exists, but the mechanism still has to be identified.

A much clearer picture exists with respect to ELMs. As expected for ideal ballooning, $\nabla p_{e,max} \propto I_p^2$ for type I ELMs. ∇p_e is significantly below $\nabla p_{e,max}$ for type III ELMs. The occurrence of ELM types depends on edge T_e , but not density. Consistent with resistive modes, type III ELMs are found at lower T_e than type I ELMs.

References

- [1] Itoh, K. and Itoh, S.-I. 1996 *Plasma Phys. Contr. Fus.* **38**, 1
- [2] Ryter, F., II-Mode Database Working Group 1995 IPP-4/269
- [3] Carlstrom, T. N., 1995 IAEA H-Mode workshop, Princeton, GA-A22191
- [4] ASDEX Team, 1989 *Nucl. Fusion* **29**, 1959
- [5] Righi, E. *et al.* 1995 Proceedings of the 22nd EPS Conf. on Contr. Fusion and Plasmaphys., Bournemouth, Vol. 19C, p. II-073
- [6] Groebner, R. J., 1995 IAEA H-Mode workshop, Princeton, GA-A22184
- [7] de Blank, H. *et al.* 1996 *this conference*
- [8] Kallenbach, A. *et al.* 1995 Proceedings of the 22nd EPS Conf. on Contr. Fusion and Plasmaphys., Bournemouth, Vol. 19C, p. II-005
- [9] Doyle, E. J. *et al.* 1991 *Phys. Fluids* **B3**, 2300
- [10] Suttrop, W. *et al.* 1995 Proceedings of the 22nd EPS Conf. on Contr. Fusion and Plasmaphys., Bournemouth, Vol. 19C, p. III-237
- [11] Zohm, H. 1996 *Plasma Phys. Control. Fusion* **38**, 105
- [12] Gohil, P. *et al.* 1995 *Phys. Rev. Lett.* **61**, 1603
- [13] Zohm, H. *et al.* 1995 *Nucl. Fusion* **35**, 543
- [14] Wesson, J. 1987 *Tokamaks* (Oxford), p. 156